	Dok.nr. / Doc.No.	Utg. / Rev.	Sida / Page
	50029813	**B**	1(13)

Dokumentnamn / Title Specific Absorption Rate (SAR) Analysis for SJM RF implants with embedded antenna			
Avdelning / Dept. UDET	Utfärdare / Originator Andreas Kronhamn		Ersätter / Supersedes A
Avser / Concerns RF Device Project		Säkerhetsklass / Classification **Intern / Internal**	Bilagor / Attachments N/A
Distribueras till / Distribution list N/A			

Utgåva / Revision	Revisionshistoria / Revisions History
A	First revision
B	Updated with close-in views of antenna region, figures in section 4.5 and clarifications.

1 Introduction

St. Jude Medical has a wireless communication system that is operating under the MICS (Medical Implant Communication Service) standard. The intended use is for communication between Implanted Medical Devices (IMD) and an, to the body, external transceiver.

This report is a summary of SAR computational modelling results to support the class II permissive change request to the current FCCID: RIASJMRF. The class II permissive change is for a new device antenna implementation introduced to all existing RF implant models. The original device loop antenna is a thin round wire on the surface of the device header. The new configuration is an embedded loop antenna with a flat wire routed inside the epoxy header.

This report covers all existing RF implant models with the three header variants, represented by *Current DR RF, Current VR RF and Promote RF* device models.

This SAR computation modelling is to show compliance to radio frequency exposure limits as defined in, 47 CFR Part1, section 1.1307 and in 47 CFR Part2, section 2.1093. The usage of the equipment is uncontrolled and hence the limit for partial-body SAR is 1.6W/kg. The partial-body SAR is averaged over any 1g tissue volume in the shape of a cube. The Whole-body limit for average SAR is 0.08W/kg.

2 Scope

The scope of this report is to support the class II permissive request to the current FCC ID: RIASJMRF and to show compliance for existing RF implant header variants, represented by *Current DR RF, Current VR RF and Promote RF*, as required in 47 CFR Part 95, section 95.603(f).

3 Summary

The computed SAR levels are well below the limits as specified in 47 CFR Part1, section 1.1307 and in 47 CFR Part2, section 2.1903.

RF implant header variants	Partial body SAR Max 1g [W/kg]	The ANSI safety limit of SAR Max 1 g [W/kg]	Whole body average SAR [W/kg]	The ANSI safety limit of whole body SAR [W/kg]
Current DR RF	0.0070	1.6	6.3E-7	0.08
Current VR RF	0.0087	1.6	6.6E-7	0.08
Promote RF	0.0066	1.6	6.2E-7	0.08

Table 1 Computed SAR value of Current DR RF, Current VR RF and Promote RF Promote RF, with embedded antenna.

4 Method

The CST Micro Wave Studio (MWS) version 2008.6-May 26 2008–22 simulation program was used during the simulations. As described in [1] FIT is identical to pure FDTD method as defined by Yee [2]. MWS is using the Finite Integration Technique (FIT) which in the time domain can be considered as a conformal FDTD method.

MWS has in order to increase computational accuracy and efficiency added features to the pure FDTD. During the simulations the Perfect Boundary Approximation (PBA)® and Thin Sheet Technique (TST)™ functionalities were used. The grid was implemented as non-homogeneous and non-equidistant.

4.1 Simulation volume

Cad models of relevant parts of the implanted device were imported to the simulator in order to enable a correct representation of the antenna function. In order to simulate a worst case scenario the IMD was put inside muscle tissue shaped as a parallelepiped measuring 175 by 114 by 178 (XYZ) mm, see figure 1. This is judged to be a worst case scenario since an alternate placement in fat will lead to lower SAR values due to the much lower conductivity and dielectric constant of fat. The boundary condition Perfect Electrical Conductor was used. The reason for using this boundary was to safeguard that all emitted energy was kept within the computational volume. The validity of the chosen parallelepiped is verified in figure 2 to figure 7, where it is found that the energy relevant for the SAR calculation is dissipated in a distance much shorter than the distance to the boundary condition. The IMD metal parts were all modeled as PEC. This is a worst case scenario since a PEC conductor is lossless and hence does not reduce SAR as would a real metal conductor. The dielectrical materials implemented in the simulator are viewed in table 2. The muscle electrical properties were retrieved from [3]. The electric properties were taken as mean value of transversal and parallel muscle fibers at 403 MHz. The density was chosen according to [4].The materials used in SAR calculations are all include as non dispersive.

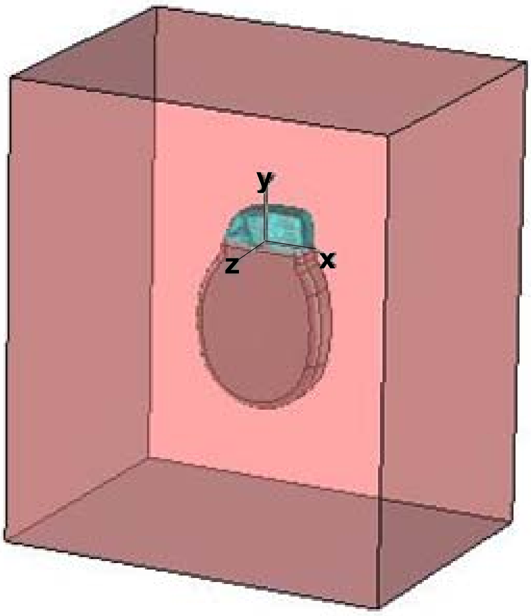

Figure 1 Device placed inside a parallelepiped of muscle. Displayed is also XYZ coordinate system

Material	Relative dielectric constant, εr	Electrical conductivity [S/m]	Density [kg/m^3]
Epoxy	3.5	0.033	N/A
Muscle	57.9	0.82	1000

Table 2 Properties of the dielectrical materials used in the simulations.

4.2 Simulated object

For all header variant simulations an imported CAD model was used and hence the model used during simulations is representative. The loop antenna, device can, casted header, all wires in the header as well as the set screw blocks are included in the CAD model. The lead cavities were filled with epoxy. The power was fed using a discrete port between device can and antenna. This is the same place as where the antenna is connected to the RF-feedthru.

4.3 Input power and source excitation

A conservative approach was used for determining the output power to be used as input to the simulation. The determination was made trough measurements of the output power emitter from RF-hybrids. A slide screw tuner [7] equipment was used to create several antenna impedance that have been seen during implant studies for the three header variants. The maximum measured output power when the RF-hybrids saw different antenna impedances was 0,63mW. The maximum output power was measured with a CW (Continuous Wave) signal. 0,63mW was subsequently used as input to the SAR calculation.

The simulated impedances, as described in 4.1, for the three header variants were a subset of the antenna impedances described above and therefore is the maximum output power considered representative for the three header variants.

A typical user scenario is that during the first 20 seconds the stored IEGM (Intracardiac Electrogram) and other device data is transferred at maximum data speed to the external device. During these first 20 seconds (Phase1) the implant has a transmit on-time duty cycle of 80%. After these first 20 seconds (Phase2) the implant is transmitting almost only real time IEGM at lower data rate. During this phase the transmit on-time duty cycle is 50%. The output power used in the SAR calculations is based on the worst case duty cycle, 0.51 mW (Phase 1).

Max measured power [mW]	Phase 1 power [mW]	Phase 2 power [mW]
0.63	0.8 x 0.63 = 0.51	0.5 x 0.63=0.32

Table 3 The power used during SAR calculations was 0.51mW (Phase 1).

The source used to excite the simulation was a voltage gap between device can and antenna at the same place where the antenna is connected to the RF-feedthru. MWS calculated SAR based on the power accepted by the antenna so no antenna impedance matching was needed.

4.4 SAR calculation

The device was modeled at the middle of the frequency band since the MICS frequency band has less than 1% bandwidth and no differences in SAR is expected between high, middle and low channels. MWS calculates 1 g average SAR using a method that is compliant with IEEE Std C95.3-2002 and described below:

- compute the losses in a cell:
  Loss_x = 0.125 (sigma_1x |E_1x|^2 + ... + sigma_4x |E_4x|^2)
  Loss_cell = Loss_x + Loss_y + Loss_z

- compute the mass of each cell (conformal integration):
  Mass_cell = dx dy dz rho_cell

- find an averaging cube with a mass of 1 g (iteratively) and integrate the losses in this cube.

The described averaging procedure is therefore a 12 component averaging and also conformal to IEEE C95.3.

The whole body SAR was calculated as the power accepted by the antenna divided by the total mass of the modeled volume.

4.5 Mesh density

MWS has a powerful mesh engine that creates mesh as a function of the object that is simulated. However a lower limit can be set on the largest allowed mesh cell in the calculation. The size of the largest allowed Mesh cell was set to a 30th wavelength in the muscle at the highest simulation frequency 600MHz. However it should be noted that the actual resolution of the IMD is much finer. The way the resolution of objects is performed is by defining the mesh line ratio limit which is the ratio between the largest and smallest distance between mesh lines. The mesh line ratio limit was chosen to 50. In order to prove that the simulation was performed in a stable region where additional mesh would not alter SAR, simulations were also performed with different mesh settings, see table 4, 5 and 6. It can here be found that SAR is stable as a function of mesh density. These findings indicate that the chosen mesh density is acceptable.

lines/ wavelength	Mesh line ratio limit	Max 1g Avg SAR [W/kg]	Max 1g Avg SAR Position x;y;z[inch]	Min mesh step [inch]	Max mesh step [inch]	Meshcells
30	50	0.0070	0.68;0.17;0.060	0.0044	0.11	3 348 180
30	60	0.0070	0.68;0.17;0.060	0.0040	0.11	3 576 040
40	50	0.0070	0.68;0.17;0.060	0.0044	0.096	4 399 104

Table 4 SAR result comparison from Current DR RF when altering mesh densities. The power that was accepted by the antenna was set to 0.51 mW.

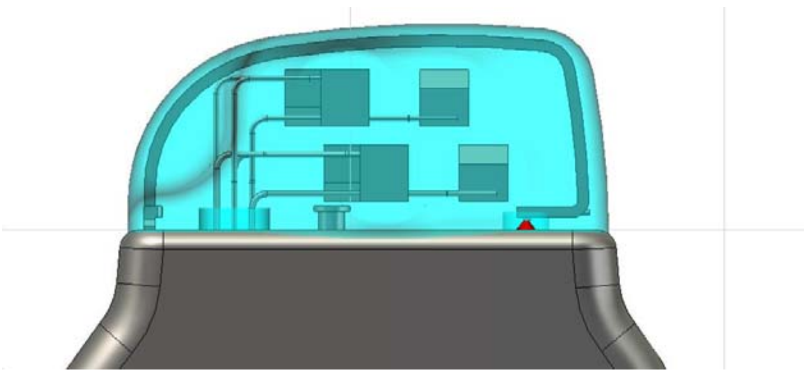

Figure 2 The header of Current DR RF. The loop antenna, device can, casted header, all wires in the header as well as the set screw blocks are included in the CAD model. The red triangle represents the feeder.

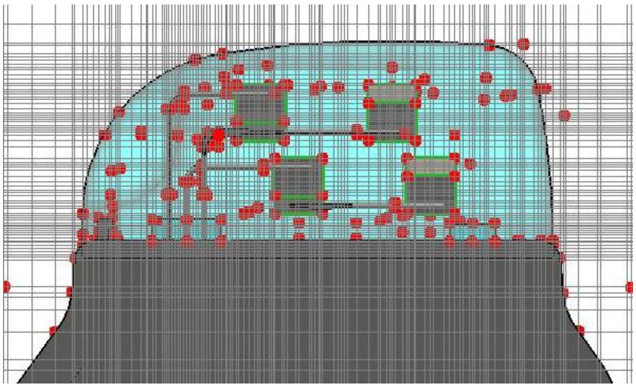

Figure 3 Mesh around the header when Current DR RF was simulated with 30 lines/wavelength and the mesh line ratio was set to 50.

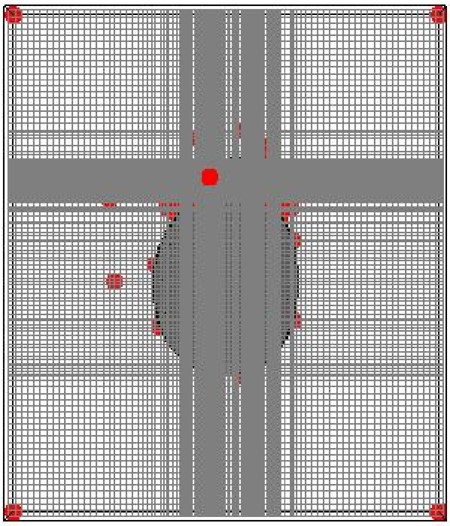

Figure 4 Mesh in the full simulation volume when Current DR RF was simulated with 30 lines/wavelength and the mesh line ratio was set to 50.

lines/ wavelength	Mesh line ratio limit	Max 1g Avg SAR [W/kg]	Max 1g Avg SAR Position x;y;z[inch]	Min mesh step [inch]	Max mesh step [inch]	Meshcells
30	50	0.0087	0.49;0.37;-0.095	0.0044	0.11	3 102 192
30	60	0.0087	0.49;0.37;-0.095	0.0041	0.11	3 320 343
40	50	0.0087	0.49;0.37;-0.095	0.0044	0.076	4 140 918

Table 5 SAR result comparison from Current VR RF when altering mesh densities. The power that was accepted by the antenna was set to 0.51 mW**.**

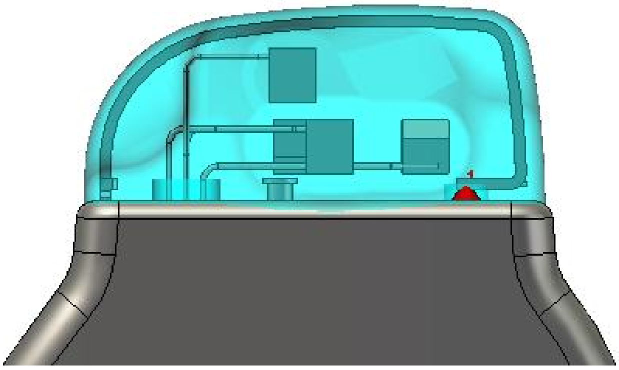

Figure 5 The header of Current VR RF. The loop antenna, device can, casted header, all wires in the header as well as the set screw blocks are included in the CAD model. The red triangle represents the feeder.

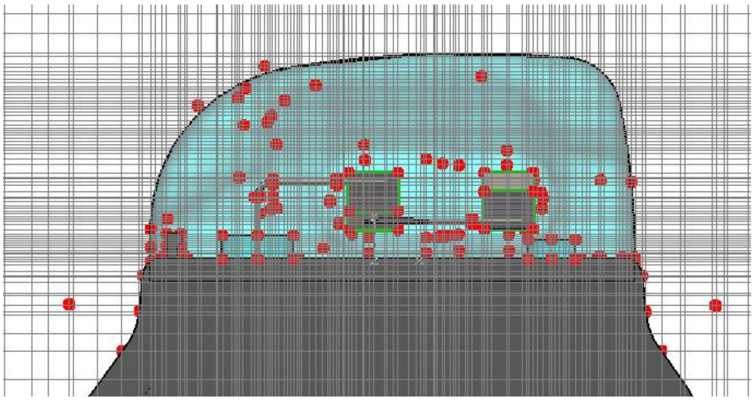

Figure 6 Mesh around the header when Current VR RF was simulated with 30 lines/wavelength and the mesh line ratio was set to 50.

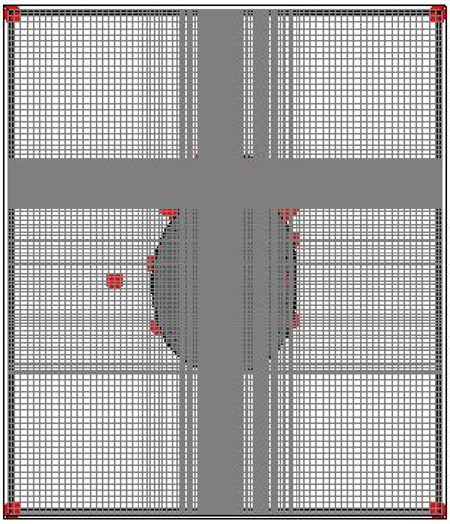

Figure 7 Mesh in the full simulation volume when Current VR RF was simulated with 30 lines/wavelength and the mesh line ratio was set to 50.

lines/ wavelength	Mesh line ratio limit	Max 1g Avg SAR [W/kg]	Max 1g Avg SAR Position x;y;z[inch]	Min mesh step [inch]	Max mesh step [inch]	Meshcells
30	50	0.0062	0.69;0.16;0.061	0.0044	0.13	2 931 483
30	60	0.0062	0.69;0.16;0.061	0.0036	0.13	3 484 956
40	50	0.0062	0.69;0.16;0.061	0.0044	0.095	4 207 526

Table 6 SAR result comparison from Promote RF when altering mesh densities. The power that was accepted by the antenna was set to 0.51 mW.

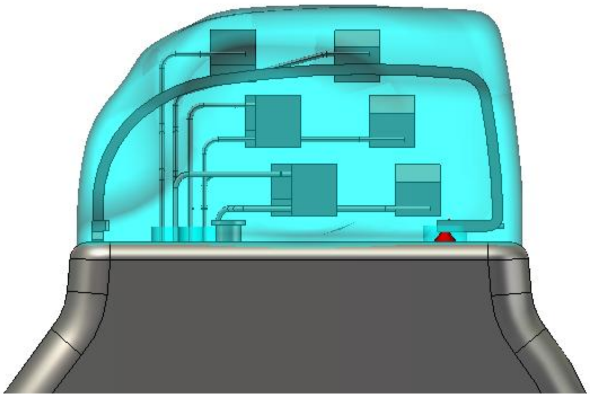

Figure 8 The header of Promote RF. The loop antenna, device can, casted header, all wires in the header as well as the set screw blocks are included in the CAD model. The red triangle represents the feeder.

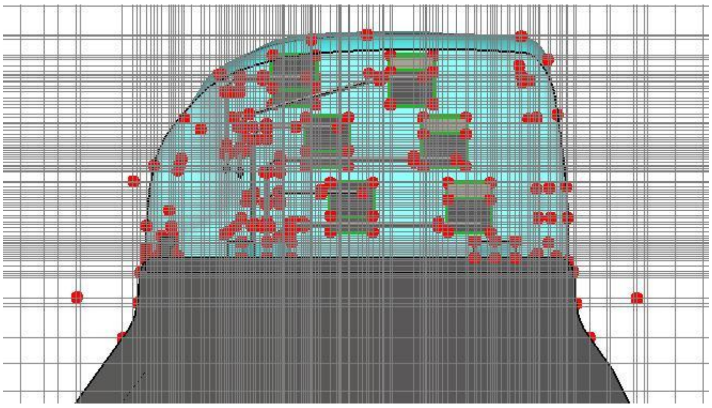

Figure 9 Mesh around the header when Promote RF was simulated with 30 lines/wavelength and the mesh line ratio was set to 50.

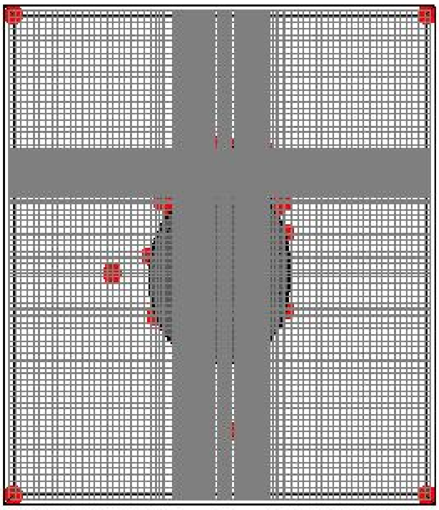

Figure 10 Mesh in the full simulation volume when Promote RF was simulated with 30 lines/wavelength and the mesh line ratio was set to 50.

5 Results

Figure 11 – 16 show the SAR distribution around the devices when antenna is fed with 0.51mW. The largest energy deposition is close to the antenna feeding port and as expected the deposition is decreasing when moving away from the antenna feed.

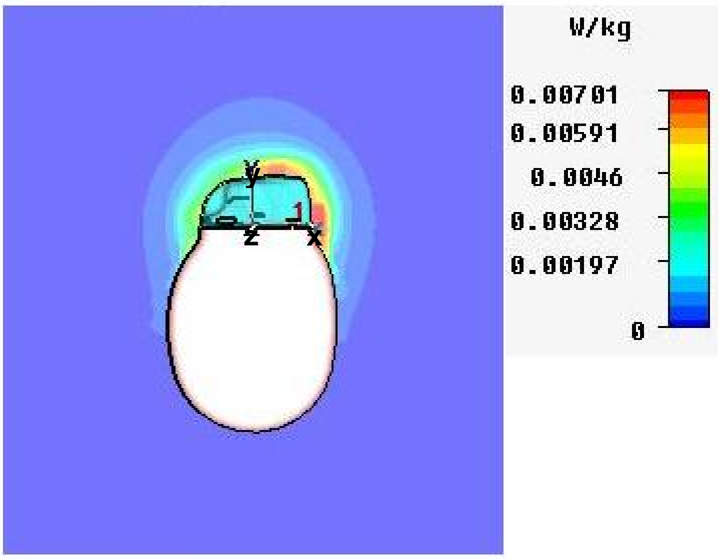

Figure 11 XY cross section of max 1g average SAR distributions, from Current DR RF, at or in close proximity to the place where the maximum SAR is found when antenna is fed with 0.51mW.

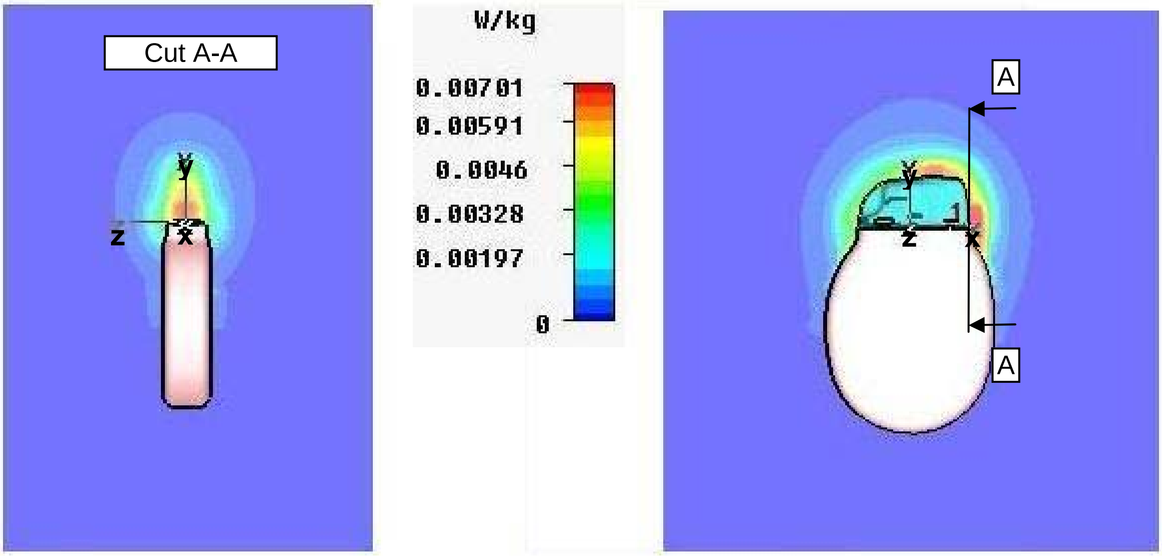

Figure 12 YZ cross section of max 1g average SAR distributions, from Current DR RF, at or in close proximity to the place where the maximum SAR is found when antenna is fed with 0.51mW

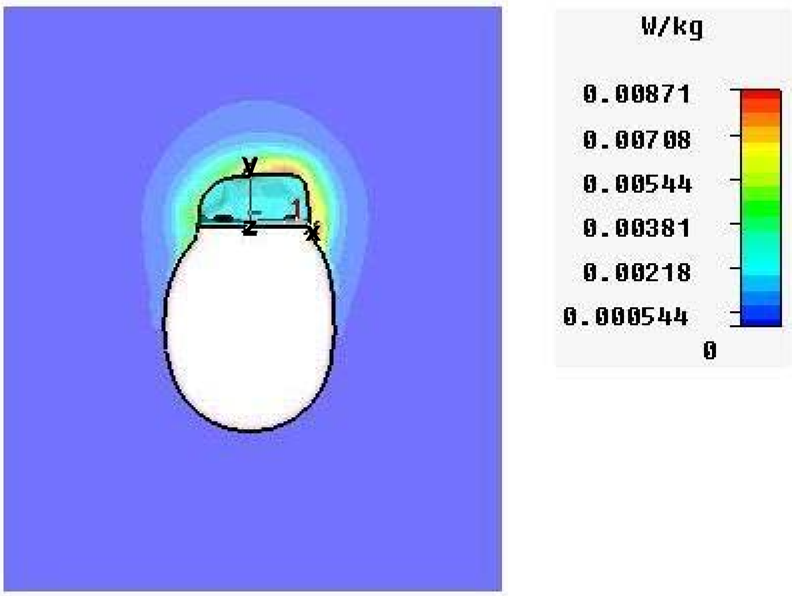

Figure 13 XY cross section of max 1g average SAR distributions, from Current VR RF, at or in close proximity to the place where the maximum SAR is found when antenna is fed with 0.51mW.

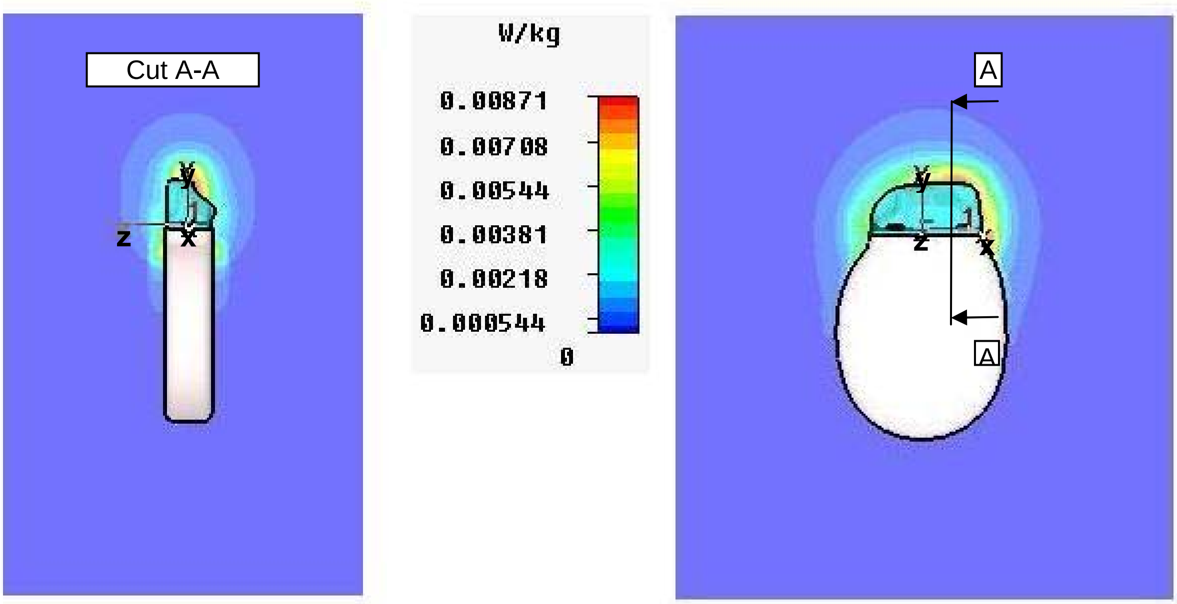

Figure 14 YZ cross section of max 1g average SAR distributions, from Current VR RF, at or in close proximity to the place where the maximum SAR is found when antenna is fed with 0.51mW.

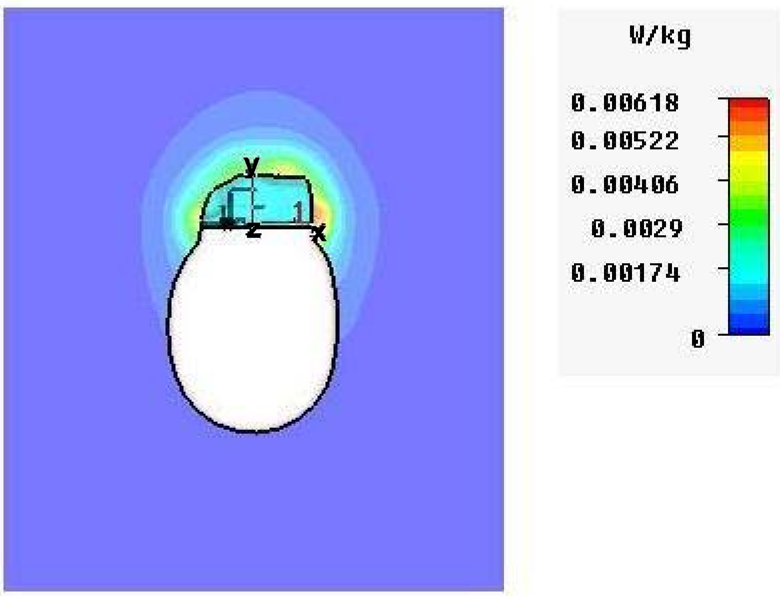

Figure 15 XY cross section of max 1g average SAR distributions, from Promote RF, at or in close proximity to the place where the maximum SAR is found when antenna is fed with 0.51mW.

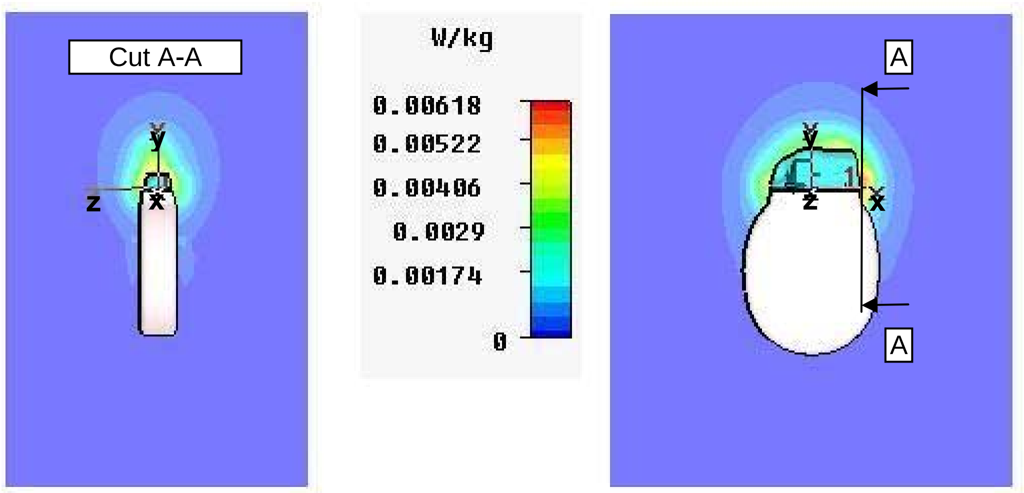

Figure 16 YZ cross section of max 1g average SAR distributions, from Promote RF, at or in close proximity to the place where the maximum SAR is found when antenna is fed with 0.51mW.

RF implant header variants	Partial body SAR Max 1g [W/kg]	The ANSI safety limit of partial body SAR [W/kg]	Whole body average SAR [W/kg]	The ANSI safety limit of whole body SAR [W/kg]
Current DR RF	0.0070	1.6	6.3E-7	0.08
Current VR RF	0.0087	1.6	6.6E-7	0.08
Promote RF	0.0066	1.6	6.2E-7	0.08

Table 7 Computed SAR value of Current DR RF, Current VR RF and Promote RF Promote RF, with embedded antenna.

6 Compliance

The results presented in section 5 table 7 are well below the limit for partial-body SAR and whole-body average SAR.

7 OET 65C

OET65C Appendix3 [4] defines the specific information needed to prove compliance. Below are listed either where to find information in the report or, in some cases, further clarifications.

7.1 Computational Resources

A 4GB RAM 490 precision DELL workstation with two 2.66 GHz Intel Woodcrest processors was used during the simulations. Operating system was Windows XP.

RF implants header variants	Mech cells	Solver memory [MB]
Current DR RF	3 348 180	1257
Current VR RF	3 102 192	1165
Promote RF	2 931 483	1101

Table 8 Solver memory requirement of Current DR RF, Current VR RF and Promote RF, with embedded antenna.

7.2 FDTD algorithm implementation and validation

See section 4.

7.3 Computational parameters

See section 4.

7.4 Phantom implementation and validation

See section 4.

7.5 Tissue dielectric parameters

See section 4.

7.6 Transmitter model implementation and validation

See section 4.

Device can, header plastics, wires and blocks in the header are important to get an accurate result.

7.7 Test device positioning

Device positioning is in the middle of the muscle parallelepiped.

7.8 Steady state termination procedures

The simulation was stopped when the energy in the whole computation volume was 50 dB below initial energy. The added error due to the truncation criteria is on average 10E-5.

7.9 Computing peak SAR from field components

See section 4.4.

7.10 One gram averaged SAR procedures

See section 4.4.

7.11 Total computational uncertainty

Since the mesh has been shown to be saturated and the truncation criteria is set to give errors on the order of 10E-5 the computational uncertainty is low. It is estimated that the total uncertainty in calculating SAR is below 10%.

7.12 Test results for determining SAR compliance

See section 5.

8 References

1. S. Gutschling, H. Krüger, T. Weiland: Modeling Dispersive Media Using the Finite Integration Technique. Proceedings of the 14th Annual Review of Progress in Applied Computational Electromagnetics (ACES 1998), Vol. 2, March 1998, pp. 832-837

2. K.S. Yee; Numerical Solution of initial boundary value problems involving Maxwells Equations in isotropic media; 1966; IEEE Transactions on antennas and propagation; Vol. 17; p. 585-589

3. http://www.fcc.gov/fcc-bin/dielec.sh; The tissue parameters provided here are derived from the 4-Cole-Cole Analysis in "Compilation of the Dielectric Properties of Body Tissues at RF and Microwave Frequencies" by Camelia Gabriel, Brooks Air Force Technical Report AL/OE-TR-1996-0037.

4. FCC OET Bulletin 65, supplement C.

5. IEEE C95.1-1999 the human exposure standard

6. IEEE C95.3 -1999 the measurement practices standard

7. Maury Microwave, operating instructions; Coaxial Manual Tuners.